Scintillating Fiber Dosimeter for Radiation Therapy Accelerator

J. M. Fontbonne, G. Iltis, G. Ban, A. Battala, J. C. Vernhes, J. Tillier, N. Bellaize, C. Le Brun, B. Tamain, K. Mercier, and J. C. Motin

***Abstract*—Radiation therapy accelerators require highly accurate dose deposition and the output must be monitored frequently and regularly. Ionization chambers are the primary tool for this control, but their size and fragility make them unsuitable for use during patient treatment. In collaboration with a French center for cancer treatment in Caen, we describe the development and testing of a low-cost radiotherapy dosimeter (SDM) based on scintillating fibers and signal processing to reduce the effect of Cerenkov radiation background. The employment of photodiodes for light collection reduces the cost relative to systems using photomultipliers (PMTs). However, we have also developed a highly sensitive system that uses PMTs for very low-dose deposition for Brachytherapy. Comparison with standard ionization chamber shows about a 1% difference over a range of 6- to 25-MV photons. This dosimeter is 1 mm in diameter and can be placed where ever required including inside the body. Its small size and flexibility make it useful for delimiting critical regions, where organs may be very radiation sensitive.**

***Index Terms*—Dosimetry, oncology, radiotherapy, scintillator.**

I. Introduction

A SCINTILLATION dosimeter is essentially a scintillation detector operated in current mode using a photomultiplier (PMT) tube, avalanche photodiode, or Si photodiode. The polymethylmethacrolate (PMMA) from which fibers are made has almost the same Z and density as human soft tissue [1], [2]. These properties ensure that the attenuation coefficient of the fibers is close to that of the patient. Moreover, the range of β particles is also comparable. Thus, the measured dose is a good measure of the delivered dose to the patient at the location of the dosimeter. The fiber is also passive, there is no high voltage, and the fiber can be directly attached to the patient.

The fiber is flexible and small enough to be used in intracavity measurements such as Curietherapy. Its flexibility and spatial resolution due to their very small diameters allow very accurate delimitation of irradiated and zero dose zones; patient alignment can effectively be controlled on-line. This can be very important in radiotherapy quality control. These devices are very inexpensive, and its use as part of a multichannel system with many measurement points in/on a patient is easily within the technology and should be cost effective.

Manuscript received November 26, 2001; revised July 2, 2002.

J. M. Fontbonne, G. Iltis, G. Ban, J. Tillier, N. Bellaize, C. Le Brun, and B. Tamain are with the Laboratoire de Physique Corpusclaire de Caen, 14050 Caen Cedex, France (e-mail: author@caelav.in2p3.fr).

A. Battala, J. C. Vernhes, K. Mercier and J. C. Motin are with the Centre Régionnal de Lutte Contre le Cancer, 14076 Caen Cedex 05, France.

Digital Object Identifier 10.1109/TNS.2002.803680

Scintillation light is proportional to the dose rate and usually has a limited range of emission wavelengths which depend on the scintillator material characteristics. The Cerenkov effect is due to the fact that electrons can exceed the velocity of light in materials with an index of refraction greater than one (almost all materials, except transparent gases). It occurs in almost every clear material at electron energies above about 180 keV [3]. Cerenkov radiation is emitted in a broad-band spectrum ranging from ultraviolet to infrared with intensity decreasing with the second power of the wavelength.

Cerenkov radiation is produced in scintillators as well as in the clear fiber optics that would be used in the scintillation dosimeter. The amount of light depends both on the dose rate and on the length of irradiated material. Thus, it will produce a bias in the dose measurement. The signal processing we have developed is designed to correct for the bias in the measurement of the scintillation light caused by the presence of the Cerenkov radiation.

II. Device Description

The scintillation dosimeter (SDM) consists of four parts.

A) The proximal sensor.
B) The main optical line from sensor to measuring box and the secondary optical line from the box to the photodetector.
C) The photodetector.
D) Signal processing.

A. The Proximal Sensor

The proximal sensor (Fig. 1) is a 2-m-long optical fiber coupled to a scintillator at one end and an FC type connector at the other. The scintillator is a Bicron BCF-60 radiation hardened scintillating fiber of l cm length, 1 mm diameter, and 7.85 mm^3 volume. The scintillator is glued to the clear optical fiber. The optical fiber is commercially available: 2-m-long, 1-mm-diameter core with 0.1-mm clear cladding and a $\phi = 2$-mm black outer covering. The FC connector is required for good optical transmissions.

B. The Main Optical Line

The primary optical fiber is 20 m long with an FC connector on each end. Because optical fibers are fragile, it is useful to protect it with a special outer cover (a flexible metal pipe for instance) to prevent damage.

The link between the primary optical fiber and the photodetector is a short optical fiber (20 cm). Despite its small length,

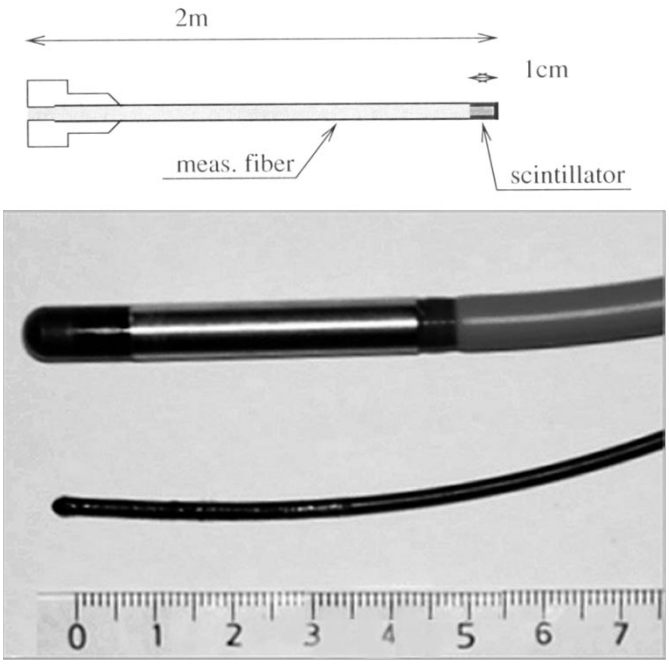

Fig. 1. Proximal sensor compared with a 0.125 cm^3 PTW ionization chamber. The scale is in centimeters.

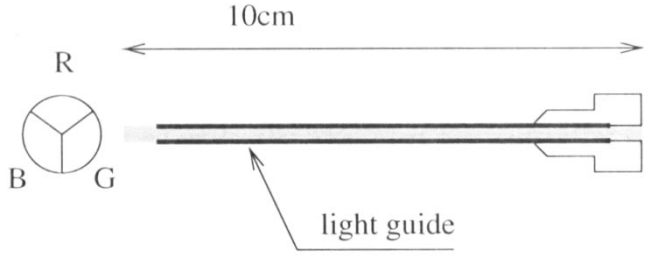

Fig. 2. The end of the optical fiber and the diode with colored filters.

it is a critical piece (Fig. 2). Problems occur in short transmission lines when twisting of the line changes the transmission efficiency and, thus, the measured dose rate. To circumvent this problem, we introduced a small radius loop at the beginning of the fiber. This loop has the effect of transmitting only small angle emission from the scintillator. As such, the subsequent transmission efficiency of the fiber is 100% irrespective of any twists or loop in it.

C. The Photodetector

The photodetector is a MAZeT GmbH product MCS3 type [4]. It consists of three p–i–n photodiodes (low capacitance) covered by interference filters (Blue, Green and Red) that correctly match our requirements.

There are several other options (depending on cost and goal) described in Table I. Despite its cost, using a PMT may lower the equivalent noise of the device a factor of ten, at least.

D. Low-Noise Analog Front-End Signal Processing

In order to reduce the noise contribution of the analog front-end electronics, we fabricated a current integrator with a resetable feedback. This integrator is made with an operational amplifier.

TABLE I
COMPARISON BETWEEN PMTS AND PHOTODIODE

	Photodetectors	
Type	PM tube	Si photo diode
Sensitivity 550 *nm*	60 *mA/W*	300 *mA/W*
drift	<0,1%/*K*	<0,1%/*K*
Dark counts eq. Noise	~100	>4000 (I_{bias}=1pA)
Thermal sensitivity	*2/5*K*	*2/10*K*
Stability over time	1%/16 *h*	0%
Linear error	2%@*80mA*	0%
Cost (1 channel)	>200 Euros	20 Euros

The feedback is a small capacitance (2 pF) in parallel with a PMOS transistor acting as a controlled resistor (low impedance $<$ kΩ or high impedance $>$500 GΩ). The integration time $T_{\rm int}$ is selectable from 1 to 500 ms. Presently, we selected $T_{\rm int} =$ 500 ms and the noise, expressed in terms of equivalent current at the input, is about 2 $\rm fA_{rms}$ (including the photodetector noise). This kind of circuit suffers two major problems, charge injection and thermal drifts.

1) Charge Injection: In order to switch the PMOS transistor from low to high impedance, we need to apply a voltage step that induces a charge step transferred to the input of our circuit by parasitic capacitances. This phenomenon, known as charge injection, leads to the induction of several pico Coulombs bias at the input. We corrected for this injection by using a "counter injection" circuitry which sends to the input about the same amount of opposite polarity charge. In order to improve the measurements, we also implemented correlated double sampling. This circuit, known as CDS, restores the base line of the current integrator.

2) Thermal Drifts: In order to reduce noise, the front-end amplifier is an FET operational amplifier. As a consequence, the input bias current doubles every seven degrees. The input bias current of commercially available OpAmps is about 1 pA. Thus, it would be necessary to control the temperature stability to within $\pm 0.01^\circ$ to ensure a current drift less than ± 1 fA.

The solution we used was to add a blind channel. This blind channel controls the dark current of a photodetector (the same as the active channels). Of course, the input bias current is different from one OpAmp to another, but for a short period of time (tens of minutes) the corresponding correlation is linear enough to ensure the correct dark current subtraction. This is the subject of the digital signal processing section.

3) Digital Signal Processing: The current measuring device consists of two photodetectors and four analog processing channels. One photodetector is used for dark current monitoring and is connected to what we call the "black" channel. The second photodetector is connected to three analog lines called Blue, Green, and Red channels.

We measure the voltage for each channel after a 500-ms integration time, leading to four data values of which only Black, Blue, and Green are used. When the beam is off, the software enables the extrapolation procedure that will run during beam on time. This extrapolation procedure consists of continuously adjusting correlation coefficients between the Black channel and the other channels.

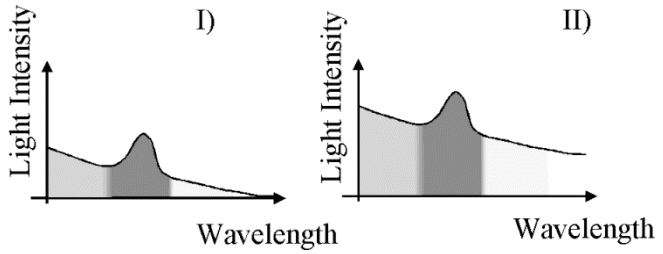

Fig. 3. Schematic spectra for different dose. The peak represents the scintillations the continuous signal represents Cerenkov radiation. I is for a small field. II is for a large field and higher dose.

Just after the beam is turned off, it is possible to use an interpolation procedure which consists of fitting the continuous level (before and after beam on) of colored channels with the Black channel. Then, the dark current subtraction is performed.

This procedure is more efficient than extrapolation but cannot run while the beam is on. Our measurements showed that when temperature equilibrium is achieved, the extrapolation and interpolation procedures led to similar results.

III. Cerenkov Cancelation-Calibration

For the SDM, Cerenkov radiation is produced both in the scintillating fiber (SF) and in the optical fiber (OF); the overall signal is, therefore, a function of the length of irradiated OF. We have been able to resolve the Cerenkov and scintillation contributions because of the difference in emitted light wavelength, and narrower range of emission wavelength for the SF. The discrimination is achieved by filtering the light signal with two filters (the diode has these filters).

The corresponding G (resp. B) Green (resp. Blue) contributions are linked to the measured dose D in a linear relationship. The calibration procedure allows the user to convert electrical units into radiological units. If we use the Cerenkov effect subtraction, we need two calibration points to determine the difference between scintillation and Cerenkov light. These requirements are realized by using an ionization chamber as an absolute dosimeter and making two separate measurements (Fig. 3).

1) Small field (10 cm by 10 cm), with the sensitive area of the SDM at the middle.
2) Large field (40 cm by 40 cm), with several turns of clear fiber in the radiation field. The exact length of fiber put in the field is not important. It should just be larger than the greatest length the user will ever need (1.5 m, for instance).

Since the Scintillation and Cerenkov effect are not correlated and the amount of light linearly depends on these effects, it is possible to determine each contribution. If $G1$, $B1$, $D1$ are the signals and dose measured for calibration point 1 and $G2$, $B2$, $D2$ for point 2, one can conclude that

$$\begin{pmatrix} G1 & B1 \\ G2 & B2 \end{pmatrix} * \begin{pmatrix} kg \\ kb \end{pmatrix} = \begin{pmatrix} D1 \\ D2 \end{pmatrix}.$$

The calibration procedure allows the computation of kg and kb coefficients and then one can use the relation

$$D = kG * G + kB * B.$$

TABLE II
Typical Diode Current During Irradiation

	Green	Blue
Scintillation ($1cm$)	$20\ fA/mGy.s^{-1}$	$2\ fA/mGy.s^{-1}$
	$20\ pC/Gy$	$2\ pC/Gy$
Cerenkov	$0.2\ fA/mGy.s^{-1}.cm^{-1}$	$0.1 fA/mGy.s^{-1}.cm^{-1}$

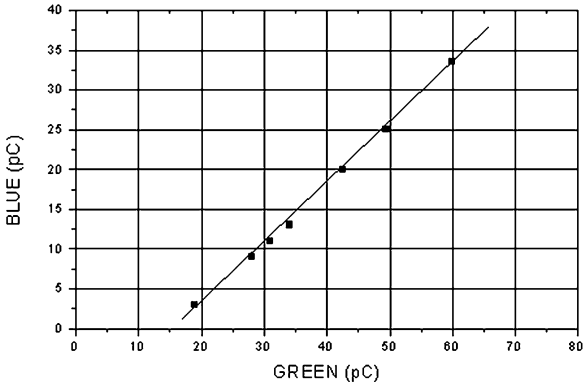

Fig. 4. Linear dependence between the blue and green emission as the length of optical fiber irradiated increases.

IV. Measurements

Several experiments were performed to validate the SDM concept.

A. Sensitivity

In order to measure the sensitivity of our device, we irradiated it with a 10 cm by 30 cm field with the scintillating part in and out of the irradiation field. The beam conditions were Beam × 15 MV, dose 1 Gy, field 10 cm by 30 cm; Ionization Chamber ($k = 1.102$) at isocenter below 2.5 cm, PMMA phantom (electronic equilibrium); SDM below 1.5-cm phantom

Table II shows orders of magnitude of the measured current. Our current integrator delivers a voltage which, expressed in MV, corresponds to fA.

The noise of "colored" channels is about 2 $\mathrm{fA_{rms}}$. Expressed in terms of radiological units, the rms dose rate noise is about 170 $\mu\mathrm{Gy} \cdot \mathrm{s}^{-1}$ (i.e., 10 $\mathrm{mGy} \cdot \mathrm{min}^{-1}$).

The scintillation figures are given for our 1-cm-long scintillator. They are given to provide an order of magnitude and more accurate conversion factors are obtained from the calibration procedure. We have several (more or less expensive) solutions to improve the signal to noise ratio and achieve lower dose rate measurements.

1) Use of PM tubes [5]. This solution has been adopted for low-dose deposition treatment such as Brachytherapy or radiological exams. The PMTs are filtered for wavelength discrimination.
2) Gluing a small piece of aluminum at one end of the scintillator doubles the scintillation light, but does not affect Cerenkov light.

B. Irradiation Length Linearity

To show that the amount of light in the green channel linearly depends on the amount of light in the blue channel for the Cerenkov effect, we irradiated several lengths of fiber ranging

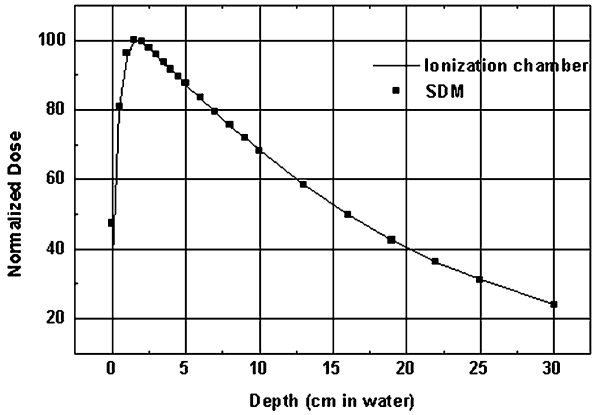

Fig. 5. Depth dose measurement comparison between SDM and a 0.125-cm PTW ionization chamber. 6-MV photons.

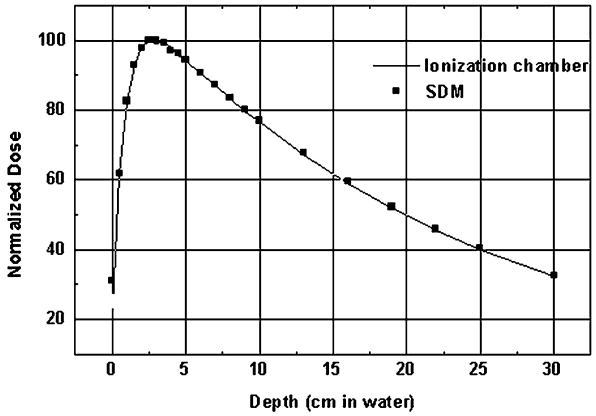

Fig. 6. Depth dose measurement comparison between SDM and a 0.125-cm PTW ionization chamber. 15-MV photons.

from 5 to 140 cm (Fig 4). The beam conditions were Beam $\times$ 15 MV; dose 1 Gy; field 10 cm $\times$ 30 cm; Ionization Chamber $(k = 1.102)$ at isocenter below 2.5 cm, PMMA phantom (electronic equilibrium); SDM below 1.5-cm phantom.

C. Optical Line Mounting Reproducibility

We calibrated the device and then completely dismounted and remounted it (proximity sensor, main optical line) several times to show that delivered the dose indication did not change.

Beam conditions: Beam $\times$ 15 MV, dose 1 Gy, field 10 cm $*$ 10 cm; I.Ch $(k \sim 1.102)$ and SDM at isocenter below 2.5 cm PMMA phantom (electronic equilibrium).

The measured dose was within $\pm 0.8\%$ of that measured by the ionization chamber.

D. Depth Dose Measurements at Several X Beam Energies

We have shown that the dose measured in a water phantom at different depths with the SDM is linearly related to the to that of a 0.125 cm^3 PTW ionization chamber. Beam conditions: Beam X 6 MV, 15 MV, 24 MV, dose 0.5 Gy maximum; field 10 cm $\times$ 10 cm; phantom water surface DSP100.

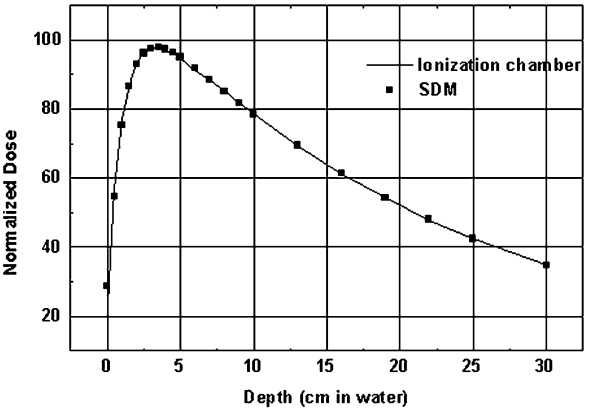

Fig. 7. Depth dose measurement comparison between SDM and a 0.125-cm PTW ionization chamber. 25-MV photons.

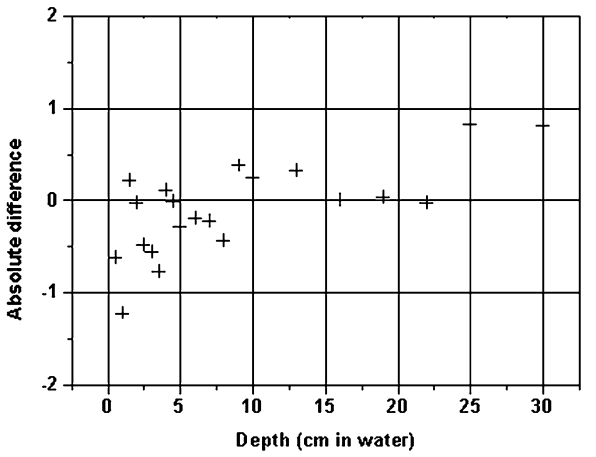

Fig. 8. Dose reading difference between the SDM and the ionization chamber with 6-MV photons. Cross-calibration.

We can see in Figs. 5–8 that the dose measured with the SDM was within $\sim \pm 1\%$ of the dose measured by the ionization chamber for depths ranging from 0.5 to 30 cm. The point at the water surface was excluded from these statistics.

E. Cross-Calibration Influence

Two points must be checked to determine whether a calibration point made at one X-ray energy is valid at other energies.

1) Do calibration coefficients depend on irradiated fiber length (it could be so if Cerenkov removal depends on beam energy)?
2) Do calibration coefficients depend on irradiation depth in a water phantom (as far as the physical phenomena depend on beam energy, the response of the SDM could change)?

Beam conditions: same data set as in depth dose measurement section.

Table III shows that the use of one calibration made at one energy does not affect the SDM dose reading at another energy.

TABLE III
DIFFERENTIAL DOSE ERROR BETWEEN TWO CALIBRATION POINTS

		Calibration at		
		6 *MV*	15*MV*	24*MV*
X Beam	6*MV*	0%	0.6%	0.2%
	15*MV*	0.6%	0%	0.5%
	24*MV*	0.2%	0.5%	0

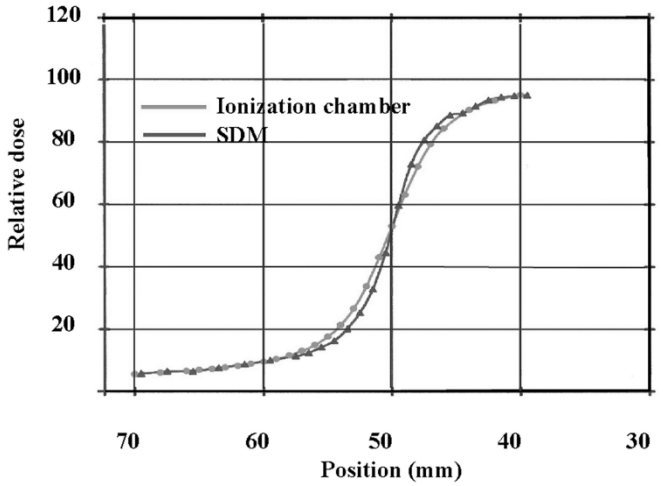

Fig. 9. Normalized dose reading versus displacement across the irradiation field frontier.

The calibration coefficients do not depend on the length of irradiated fiber or the depth in water phantom.

These measurements have shown that the dose reading on the SDM does not need to be recalculated, as it must be with a ionization chamber, when the beam energy changes.

F. Spatial Resolution

For area delimitation in certain applications, the SDM must have good spatial resolution [6]. We stepped across the radiation field with an ionization chamber and the SDM. The spatial resolution was found to be on the order of a few millimeters, and better than the ionization chamber (Fig. 9).

V. CONCLUSION AND OUTLOOK

The SDM is well suited for photon dose measurements for therapy accelerators. Its low cost, flexibility, and robustness make it suitable as an alternative tool as a substitute for ionization chambers. It is especially well suited for localized *in vivo* measurements where a chamber cannot be used. Multipoint sensors for low-dose exams such as radiology are under development as well as validation of its use with electron beams.

REFERENCES

[1] A. S. Beddar, T. R. Mackie, and F. H. Attix, "Water equivalent plastic scintillation detectors for high energy beam dosimetry: *I* physical characteristics and theoretical considerations," *Phys. Med. Biol.*, vol. 37, no. 10, pp. 1183–1900, 1992.

[2] ——, "Water equivalent plastic scintillation detectors for high energy beam dosimetry: II properties and measurements," *Phys. Med. Biol.*, vol. 37, no. 10, pp. 1901–1913, 1992.

[3] ——, "Cerenkov light generated in optical fibers and other light pipes irradiated by electron beams," *Phys. Med. Biol*, vol. 37, no. 4, pp. 925–935, 1992.

[4] *MAZeT GmbH, MCS3A Data Sheet*, Erfurt, Germany.

[5] D. Fluhs, M. Heinz, F. Indenkäpen, and C. Wieczorek, "Direct reading measurement of absorbed dose with plastic scintillators. The general concept and applications to ophthalmic plaque dosimetry," *Med. Phys.*, vol. 23, no. 3, 1996.

[6] A. S. Beddar, T. J. Kinsella, A. Ikhef, and H. Sibata, "A miniature scintillator-fiberoptic-PMT detector system for dosimetry of small fields in stereostatic radiosurgery," *IEEE Trans. Nucl. Sci.*, vol. 48, pp. 924–928, June 2001.